RESEARCH: TISSUE ENGINEERING

APPLICATION OF DEXTROSCOPE VIRTUAL REALITY SYSTEM IN ANATOMICAL RESEARCH OF INNER STRUCTURES IN PETROSAL BONE

De-Lin Yang[1], Xiao-ming Che[1], Mei-qing Lou[2], Qi-Wu Xu[1], Jin-Song Wu[1], Wen-sheng Li[3], and Da-Ming Cui[2] *

[1]*Dept. of Neurosurgery, Huashan Hospital, Shanghai Medical College, Fudan University, Shanghai– 200040, CHINA*
[2] *Dept. of Neurosurgery, Shanghai Tenth People's Hospital, Tongji University, Shanghai–200072, CHINA*
[3]*Anatomy Dept., Shanghai Medicine Institute, Fudan University, Shanghai–200032, CHINA*

ABSTRACT

OBJECTIVE: *To evaluate the application of virtual reality technology in anatomical study of inner structures of petrosal bones, the comparison of three dimensional (3-D) virtual microanatomy and actual microanatomy of petrosal bone was carried out.* **METHODS:** *The experiment was divided into two groups, virtual group and corpus group, each group with 20 cases. In the virtual group, images data of cadaver heads were loaded into Dextroscope workstation and dissecting of the virtual petrosal bone was simulated. In the corpus group, actual dissecting of petrosal bone on the cadaver heads was examined under microscope correspondingly. Compare the data of locating internal auditory meatus, cochlear and internal carotid artery in each group.* **RESULTS:** *The distances from the projecting point on petrosal crest of anterior margin of internal auditory orifice to the intersection of arcuate eminence and petrosal crest, and the midpoint of superior margin of external auditory orifice were 24.23 ± 2.88mm and 40.65±4.48mm in the virtual group respectively, 23.62±2.82mm and 39.35 ± 4.83mm in the corpus group respectively (P＞0.05). The distances from the anterior margin of cochlea to the root of zygomatic arch and geniculate part of internal carotid artery were 27.15±3.25mm and 4.15±0.52 mm in the virtual group; 28.35±4.05mm and 4.50±0.54mm in the corpus group respectively (P＞0.05). The distances from the petrosal crest to the anterior margin of the three sub-segments were 12.20±1.42mm, 8.63±0.94mm, and 5.42±0.63mm in the virtual group respectively; 10.68±1.24mm, 8.62±0.92mm and 5.69± 0.61 mm in the corpus group respectively (P＞0.05).* **CONCLUSIONS:** *The data measured in the virtual group was highly coincided with those data in the corpus group. Virtual anatomy of petrosal bone realized by virtual reality technology is reliable.*

[I] INTRODUCTION

With continuous improvement of computer image processing technology and corpus specimen processing technique, visible human project (VHP) have undergone from data collection at initial stage to education in medicine school with virtual three dimensional (3-D) specimen reconstructed from volumetric data [1-9], and some reports on anatomical structures of petrous bone based on the VHP data set were seen on some journals [10-15]. However, it seemed there was no report which virtual reality (VR) technique was used to research the individual anatomy of inner structures in petrous bones in skull base operation approach. This study was to explore the liability and value of VR technology in individual labyrinthine anatomy studies.

[II] MATERIALS AND METHODS

Perfusion of adult head specimens 20 set, microsurgical anatomy of equipment set, Dextroscope Workstation (Volume Interactions Co. Ltd., Singapore), software Version 1.01R; 3.0-T whole-body MRI scanner (General Electric Medical Systems, GE Signa VH/i); SOMATOM Sensation 64-slices CT scanner (Siemens AG).

2.1. Groups and topical anatomy

The experiments were carried out in the two groups respectively, virtual group with 20 clinical cases (40 hemispheres) whose lesions did not involve the petrosal bone and corpus group with 20 sets head specimen (40hemispheres). Micro topical anatomical dissections including internal auditory meatus, petrosal internal carotid artery and cochlear were done on the Dextroscope workstation in clinical patients' data. Actual anatomical dissections were correspondingly done the specimen. The total process of virtual dissection of petrous bone were taken by inner camera in blue red forma in virtual groups and measurements results were compared with data from actual anatomical dissection under microscope.

2.2. Image data acquisition

The scanning of patients were scheduled 1-3 days before operation, images data of were transferred to Dextroscope laboratory by optic disc. CTA was performed on the 64-slices CT scanner following the intravenous contrast agent injection. CTA were obtained contiguous as axial, 1-mm slices (FOV＝240mm×240mm; matrix size=256×256), Horizontal scanning range from 2nd cervical vertebrate body to the cranial top.

VR Anatomy In Dextroscope, co-registration of cranium segmented from head CT and internal carotid arteries from enhanced MR was done. The inner structures such as internal auditory meatus, cochlear and semicircular canals were showed by regulating threshold. Find the landmarkers and measure the distances corresponding to topical anatomy described in above text.

2.3. Statistical analyses

SPSS12.0 software was applied in the late stage. Paired T test checked quantitative data. RIDIT analysis checks numeration data. If value of P was less than 0.05, it demonstrated significant difference in the test.

Table: 1. The related measurement of internal auditory orifice and its surrounding structures

Groups	Virtual group (n=40)	Corpus group (n=40)	P– value
Dis. From Projecting point on the crest of Ante. Mar. of IAO to intersection of AE & crest	24.23±2.88mm	23.62±2.82mm	0.62
Dis. Bet. Projecting points on crest of Ante. Mar. of IAO & midpoint of ante. Mar. of EAO	40.65±4.48mm	42.15±5.13mm	0.75
Length of ante. Wall of IAO	11.68±1.54mm	11.55±1.30mm	0.65
Angle bet. Ante. wall of IAO & axon of the crest	43.56±4.62°	45.68±5.51	0.70

Dis, distance; Ante, anterior; Mar, margin; IAO, internal auditory meatus; EAO, external auditory meatus

[III] RESULTS

3.1. Measurements of internal auditory meatus

The Results of related measurement of internal auditory orifice and its surrounding structures were referred to **[Table–1]**. There were no significant differences between the measurements in two groups.

3.2. Measurement of cochlear

The cochlear is deeply sited in petrous bone. On the level of the crest of internal auditory meatus, the distances between anterior margin of cochlear and the root of zygomatic arch root and middle points of superior margin of external auditory meatus were 28.54±3.85mm and 27.15±3.25mm respectively **[Figure–1]**. The results of related measurements were referred to **Table–2**. There were no significant differences between the measurements in two groups.

3.3. Measurement of petrosal segment of internal carotid artery (ICA)

The petrosal segment of ICA was divided into three subsegments according to its relationship with trigeminal semiganglion, lateral segments of trigeminal ganglion (S1), segments of trigeminal ganglion (S2), and internal segments of trigeminal ganglion **[Figure–2]**. Distance between each subsegments of petrosal ICA and crest and thickness of bones on the petrosal ICA **[Table–3]**. There were no significant differences between the measurements in two groups.

Tab: 2. The distance from cochlear and its surrounding structures

Group	Virtual group (n=40)	Corpus group (n=40)	P– value
Angle Bet. the line of Internal Mar. of Co. to Ante. Mar. of IAO and crest	59.48±7.18°	61.56±7.24°	058
Dis.Bet.fundi of Co. and midpoint of superior Mar. of EAO	27.15±3.25mm	28.35±4.05mm	0.62
Dis.Bet. internal Mar. of Co. and geniculate part of ICA	4.15±0.52mm	4.50±0.54mm	0.60

Dis, Distance; Bet, Between; Mar, margin; IAO, internal auditory meatus; EAO,external auditory meatus; Co. cochlear
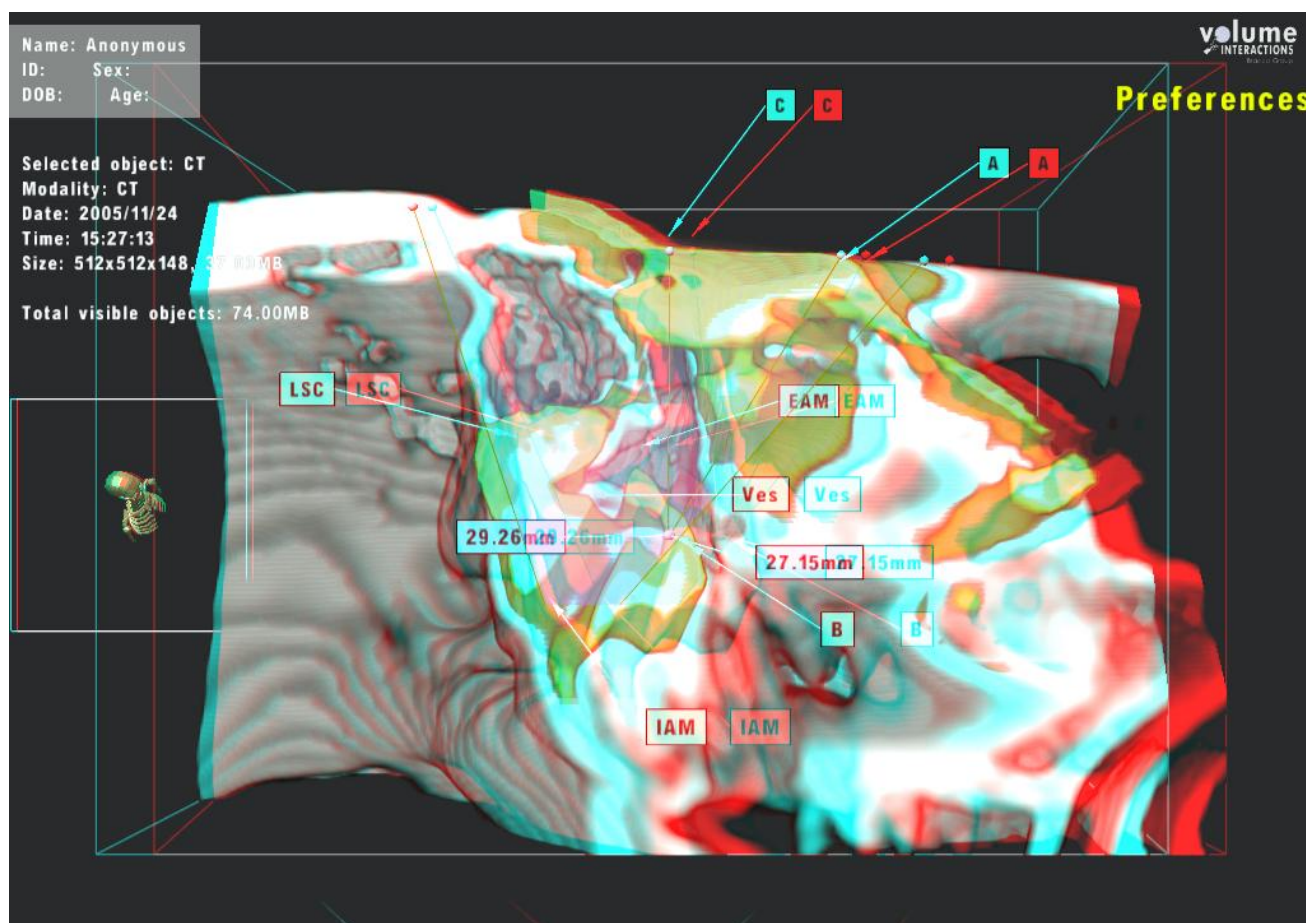

Fig: 1. The demonstration and related measurements of internal auditory meatus and cochlear A: the root of zygomatic arch; B: Lateral point of cochlear; C: midpoint of superior margin of external auditory orifice; IAM: internal auditory meatus; LSC: lateral semicircular canal; EAM: external auditory meatus; VES: vestibule; Line AB showed the interior boundary of cochlear.

Table: 3. Distance between each subsegments of petrosal ICA and crest and thickness of bones on the petrosal ICA

Group	Virtual Group (n=40)	Corpus group (n=40)	*P* –value
Dis. from S1 midpoint to crest	12.20±1.42mm	10.68±1.24 mm	0.55
Dis. from S2 midpoint to crest	8.63±0.94 mm	8.62±0.92 mm	0.58
Dis. from S3 midpoint to crest	5.42±0.63 mm	5.69±0.61 mm	0.60
T. of bone on Ante. Mar. of S1	3.22±0.37 mm	3.16±0.33 mm	0.62
T. of bone on Ante. Mar. of S2	3.05±0.31 mm	3.09±0.32 mm	0.54
T. of bone on Ante. Mar. of S3	2.28±0.23 mm	2.30±0.25 mm	0.67
T. of bone on Post. Mar. of S1	5.63±0.58 mm	5.82±0.61 mm	0.78
T. of bone on Post. Mar. of S2	3.58±0.41 mm	3.52±0.38 mm	0.69
T. of bone on Post. Mar. of S3	3.10±0.31 mm	3.23±0.35 mm	0.66

T, Thickness; Post, Posterior; Ante, anterior; Mar, margin; Dis, distance.
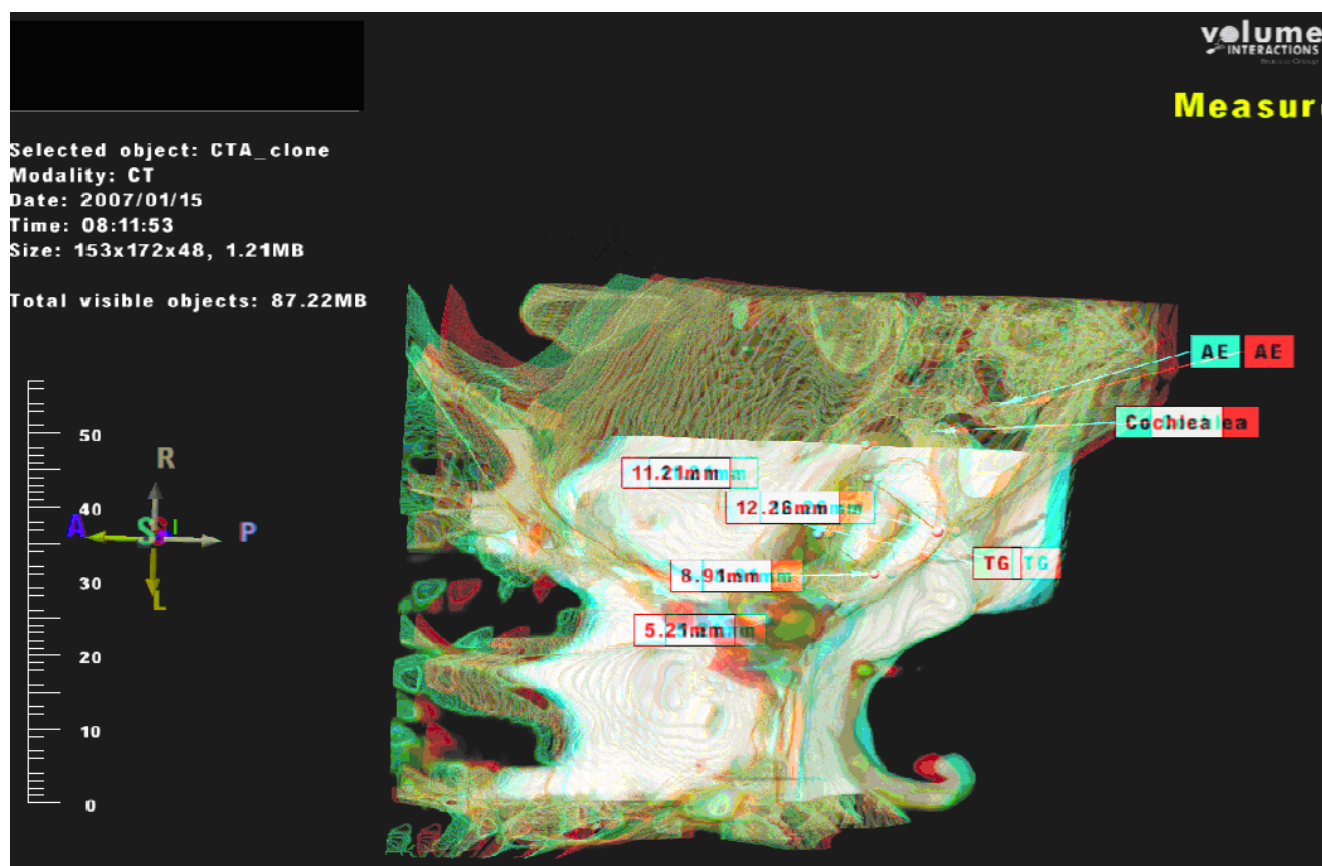
Fig: 2. The measurements of each sub segments of petrosal ICA. S1, S2, and S3 stand for three Sub segments of petrosal ICA from outwards to inwards.TG, trigeminal ganglion; AE, Arcuate eminence.

[IV]DISCUSSION

Virtual Reality (VR) technology is a comprehensive synthesized technology which can produce three dimensional virtual realistic interfaces in which people can interact with complex data in immerse environment by proper instruments. This has been used in anatomical research and education in medicine, such as the USA visible human project (VHP), voxel man reconstructured from it and reconstructed research on temporal bone from visible Chinese Man data base [1-5, 8, 9, 16-18]. However, due to lack the changes of intensity of CT and MRI signals, the quality of reconstruction images were not very desirable and visible man researches were confined in normal corpus study which just could be used in medicine education, rather not extend to guide an actual individual procedures.

Dextroscope VR workstation provided a strong tool for individual anatomical study and clinical individual procedures approach [19-24]. The study of individual anatomy of inner structures in petrous bone by Dextroscope is to explore the reliability of virtual reality technology in anatomical researches and provide more evidences for clinical applications.

Precisely understanding the anatomy of petrous bone is crucial importance in dealing with tumors involved the petrous bones. When the approach of transtemporal transtenterium was used dealing with meningioma on the apex of petrous bone, especially the tumor on the posterior fossa, grinding the apex became one of keys to total removal of tumor. Therefore, there were many reports about methods on how to grind the apex in 90s [25-30]. The basic method depends on the landmarks of inner structures in petrous bone in middle cranial fossa, but they were all roughly and lack of accuracy in location. The safety way to grind petrosal apex away included advanced driller and skillful manipulation of driller et al, the most basic point is to how to acquire the individual data about petrous bone to help locate the important inner structures such as cochlear, internal auditory meatus, semicircular canal and petrosal segment of internal carotid artery because there were great variation of structures in this area.

4.1. Location of IAM and its courses

There were two ways to locate the position of IAM. One way is according to the bisector of the angle between inferior major petrosal nerve and arcuate eminence which is roughly course of IAM. Another way is to draw a 45-degree angle along the crest from the projection point on the petrosal crest of anterior margin of IAO. Another edge of the angle is the course of internal auditory meatus. The first way can be used in epidural approach, not for subdural approach. The second way sometime failed to variation of the angles. In the experiment, we found that there was great variance in the angle between IAM and the crest. If this method was used in each patient whose apex would be ground away in operation, it probably result the damage of cochlear or IAM. It is very essential to gain the individual data

of the position of inner structures in petrous bone before operation. Actually, we used virtual reality technology to measure the individual data of the angle and design individual procedure protocol to avoid damaging of important inner structures.

4.2. Location of cochlear

It is very difficult to precisely locate the position of cochlear due to its deeply situated in petrous bone. The position of cochlear roughly used to be localized by the triangle determined by anatomical landmark on the middle fossa in past anatomical researches. Day and Fukshima[25] firstly used the anterior triangle of internal auditory meatus to locate cochlear, which is composed of anterior margin of IAM, geniculate part of ICA and geniculate ganglion where cochlear deeply situated laterally to the triangle. liu Jun[31] modified the triangle by replacement of geniculate part of ICA with midpoint of line from geniculate ganglion to spinal foramen to where cochlear deeply situated laterally. Above methods mentioned, it was feasible to locate cochlear by anatomical landmark, however lack of accuracy and individuality.

The magnified cochlear by virtual reality technology we found that cochlear situated cross the mark line of the IAM **[Figure– 1]**. If grinding apex went along the line, it would be great possible to destruct the cochlear. So if precise location of cochlear before operation was made, the map to grind petrous bone apex away would be more feasible. Our study demonstrated that at the level under superior wall of IAM 2mm, the cochlear sits medially to the fundi of IAM. The distance from internal auditory orifice to cochlear is 13.56±1.65mm or so and the distance to geniculate part of ICA 4.15±0.52mm. The angle between the line from anterior margin of IAM to anterior margin of cochlear and the crest is 59.48± 7.18°. Individual data such as distances between the fundi of cochlear and the root of zygomatic arch, from internal margin of cochlear to anterior margin of internal auditory orifice and geniculate part of ICA can be acquired by virtual reality without any damage to those structures. In operation, these data help us to locate the inner structures position precisely to reduce hearing loss resulted from imprecise location of cochlear.

4.3. Location of petrosal segment of ICA

The location of petrosal segment of ICA is very critical in operation which involved in middle fossa. The judgments of its position used to be drawn from the distance between the groove superior of petrosal nerve (GSPN) and the crest. It was reported that the distance was usually about 12mm or so. However, the actual situation is not entirely the case. The data about the distance we gained on workstation sometimes quite different from above mentioned. So we investigate the thickness of bone on the artery and also its distances. According to the position relationship between petrosal segment of ICA and trigeminal ganglion, the petrosal segment was in divided into three subsegments: lateral segments of trigeminal ganglion (S1), segments of trigeminal ganglion (S2), and internal segments of trigeminal ganglion. In virtual group, the thickness of bone

covered on the arteries became thinner from posterior to anterior as it is similar in corpus group (P>0.05). There was also no significant difference in the distance from the midpoint of each subsegment of ICA to the crest between the two groups. The results mentioned above can show as followed: 1 the data measured in virtual group was not quite same to that in corpus group; however there was no significant difference after statistical treatment. So the data in virtual group can demonstrate actual situation, and they are also individually actual situation. 2 Petrous bone on the ICA shaped tribody whose posterolateral part is thicker and anteromedial part is thinner. When the petrous bone especially medial apex to the trigeminal was being ground away, operator should be careful of the changes of thickness of bone covered on the ICA in case of the damage arteries.

In summary, VR technology can demonstrate the anatomical structure intuitively and individually in three dimensional. We have published papers on its clinical applications of virtual temporal bone in dealing with cerebrospinal fluid leakage [19,32,33]. However, there was some error in segmentation of anatomical structures. It is one of study keys to develop more advanced artificial intelligence software to lower the difficulty of segmentation and shorten manipulation time in future. If biomechanics feedback were added to make simulation of dissection more closed to actual anatomy under microscope, it will provide neurosurgeons more tools to study neurotomia.

AUTHOR CONTRIBUTIONS

Delin Yang, Xiaoming Che, and Meiqing Lou have contributed equally to this work.

ACKNOWLEDGEMENT

REFERENCES

[1] Ackerman MJ. [1991] The Visible Human Project. *J Biocommun* 18:14.

[2] Ackerman MJ. [1998]The Visible Human Project: a resource for anatomical visualization. *Stud Health Technol Inform* 52(2):1030–1032.

[3] Ackerman MJ. [1999] The Visible Human Project: a resource for education. *Acad Med* 74:667–670.

[4] Deutsch JC. [2006] Applications of the Colorado Visible Human Project in gastroenterology. *Clin Anat* 19:254–257.

[5] Jastrow H, Vollrath L. [2003] Teaching and learning gross anatomy using modern electronic media based on the visible human project. *Clin Anat* 16:44–54.

[6] Senger S. [1996] Incorporating visible human project data into the undergraduate anatomy and physiology curriculum. *Stud Health Technol Inform* 29:194–203.

[7] Slavin KV. [1997] The Visible Human Project. *Surg Neurol* 48:638–639.

[8] Zhang SX, Heng PA, Liu ZJ. [2005] Chinese visible human project: dataset acquisition and its primary applications. *Conf Proc IEEE Eng Med Biol Soc* 4:4168–4170.

[9] Zhang SX, Heng PA, Liu ZJ. [2006] Chinese visible human project. *Clin Anat* 19:204–215.

[10] Kockro RA, Hwang PY. [2009] Virtual temporal bone: an interactive 3-dimensional learning aid for cranial base surgery. *Neurosurgery* 64:216–229.

[11] Sorensen MS, Dobrzeniecki AB, Larsen P, Frisch T, Sporring J, Darvann TA. [2002] The visible ear: a digital image library of the temporal bone. *Orl J Otorhinolaryngol Relat Spec* 64:378–381.

[12] Sorensen MS, Mosegaard J, Trier P. [2009] The visible ear simulator: a public PC application for GPU-accelerated haptic 3D simulation of ear surgery based on the visible ear data. *Otol Neurotol*30:484–487.

[13] Trier P, Noe KO, Sorensen MS, Mosegaard J. [2008] The visible ear surgery simulator. *Stud Health Technol Inform* 132:523–525.

[14] Wang H, Merchant SN, Sorensen MS. [2007] A downloadable three-dimensional virtual model of the visible ear. *ORL J Otorhinolaryngol Relat Spec* 69:63–67.

[15] Li Xi-ping XY, Han De-min et al. [2004] Reconstruction of nasal and temporal anatomical strcutures based on chinese visible man dataset. *Chin J of Clinical Anatomy* 22(4):377–381.

[16] Toh MY, Falk RB, Main JS. [1996] Interactive brain atlas with the Visible Human Project data: development methods and techniques. *Radiographics*16:1201–1206.

[17] Xu XG, Chao TC, Bozkurt A. [2000] VIP-Man: an image-based whole-body adult male model constructed from color photographs of the Visible Human Project for multi-particle Monte Carlo calculations. *Health Phys* 78:476–486.

[18] Yuan Y, Qi L, Luo S. [2008] The reconstruction and application of virtual Chinese human female. *Comput Methods Programs Biomed* 92:249–256.

[19] Yang MD, Xu QW, Che XM, et al. [2008] Application of Dextroscope Virtual Reality Technology in Procedures of Skull Base Tumors. *Asian Journal of Neurosurgerey* 2:12–20.

[20] Kockro RA, Serra L, Tsai YT, Chan C, Sitoh YY, et al.[1999] Planning of skull base surgery in the virtual workbench: clinical experiences. *Stud Health Technol Inform* 62:187–188.

[21] Kockro RA, Serra L, Tseng-Tsai Y, Chan C, Yih-Yian S, et al. [2000] Planning and simulation of neurosurgery in a virtual reality environment. *Neurosurgery* 46:118–135.

[22] Kockro RA, Stadie A, Schwandt E, et al. [2007] A collaborative virtual reality environment for neurosurgical planning and training. *Neurosurgery* 61:379–391.

[23] Ng I, Hwang PY, Kumar D, Lee CK, Kockro RA, Sitoh YY. [2009] Surgical planning for microsurgical excision of cerebral arterio-venous malformations using virtual reality technology. *Acta Neurochir (Wien)* 151:453–463.

[24] Stadie AT, Kockro RA, Reisch R, Tropine A, Boor S, Stoeter P, Perneczky A. [2008] Virtual reality system for planning minimally invasive neurosurgery. *J Neurosurg* 108:382–394.

[25] Day JD, Fukushima T, Giannotta SL. [1994] Microanatomical study of the extradural middle fossa approach to the petroclival and posterior cavernous sinus region: description of the rhomboid construct. *Neurosurgery* 34:1009–1016.

[26] Harsh GR, Sekhar LN. [1992] The subtemporal, transcavernous, anterior transpetrosal approach to the upper brain stem and clivus. *J Neurosurg* 77:709–717.

[27] Kawase T, Shiobara R, Toya S. [1991] Anterior transpetrosal-transtentorial approach for sphenopetroclival meningiomas: surgical method and results in 10 patients. *Neurosurgery* 28:869–875.

[28] Kawase T, Toya S, Shiobara R, Mine T. [1985] Transpetrosal approach for aneurysms of the lower basilar artery. *J Neurosurg* 63:857–861.

[29] Osawa S, Rhoton AL, Jr., Tanriover N, Shimizu S, Fujii K. [2008] Microsurgical anatomy and surgical exposure of the petrous segment of the internal carotid artery. *Neurosurgery* 63:210–238.

[30] Sen CN, Sekhar LN. [1990] The subtemporal and preauricular infratemporal approach to intradural structures ventral to the brain stem. *J Neurosurg* 73:345–354.

[31] LIU Jun LG, SUN Ju-dong, et al. [2006] Anatomical study of the petrous structures in the temporal bone and its clinical significance. *Chin J of Clinical Anatomy* 24(1):21–24.

[32] Shen M, Zhang XL, Yang DL, Wu JS. Stereoscopic virtual reality presurgical planning for cerebrospinal otorrhea. *Neurosciences (Riyadh)* 15:204–208.

[33] Yang de L, Xu QW, Che XM, Wu JS, Sun B. [2009] Clinical evaluation and follow-up outcome of presurgical plan by Dextroscope: a prospective controlled study in patients with skull base tumors. *Surg Neurol* 72:682–689.